SAND79-8248
Unlimited Release

Heliostat Design Cost/Performance Tradeoffs

M. J. Fish, T. A. Dellin

Prepared by Sandia Laboratories, Albuquerque, New Mexico 87115 and Livermore, California 94550 for the United States Department of Energy under Contract DE-AC04-76DP00789

Printed November 1979

Sandia Laboratories
energy report

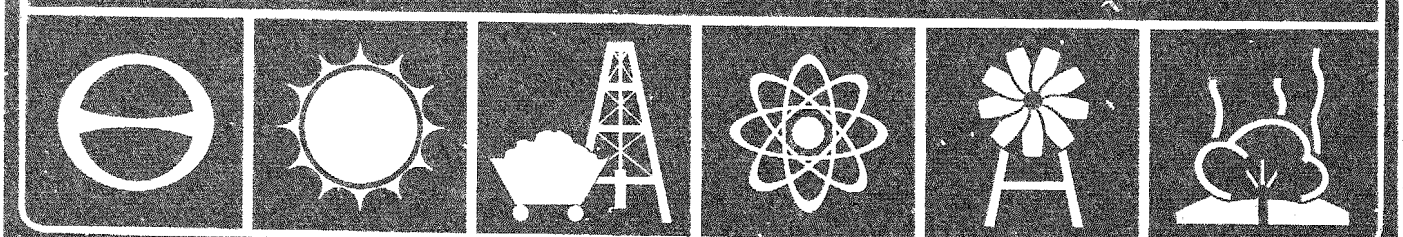

Issued by Sandia Laboratories, operated for the United States Department of Energy by Sandia Corporation.

Printed in the United States of America
Available from
National Technical Information Service
U. S. Department of Commerce
5285 Port Royal Road
Springfield, VA 22161
Price: Printed Copy $5.25 ; Microfiche $3.00

SAND79-8248
Unlimited Release
Printed November 1979

HELIOSTAT DESIGN COST/PERFORMANCE TRADEOFFS*

Miriam J. Fish
Energy Systems Studies Division

Theodore A. Dellin
Solar Components Division
Sandia Laboratories, Livermore

ABSTRACT

The heliostat field comprises the most expensive subsystem of a solar central receiver power plant. Cost reductions might be achieved by either total heliostat redesign or component substitution in existing designs. This paper discusses the value of changing any of several design specifications in the current baseline glass/metal heliostat. Results are quantified in terms of the breakeven cost; i.e., the cost of a new design which will yield the same total system energy cost as the baseline system. Changes in mirror reflectivity, pointing accuracy, surface quality, canting and focusing strategy, heliostat size, and stow requirement are evaluated.

*This work was supported by the U. S. Department of Energy under Contract DE-AC04-76DP00789.

CONTENTS

ILLUSTRATIONS

TABLES

HELIOSTAT DESIGN COST/PERFORMANCE TRADEOFFS

Introduction

A large central receiver power system utilizes a field of thousands of individually tracking heliostats to concentrate incident sunlight on a receiver at the top of a centrally located tower. Even if cost goals are achieved, the heliostat field will be the most expensive single subsystem. This is illustrated in Figure 1 in which the cost breakdown for an advanced sodium system with high reflectivity glass/steel heliostats is given [1]. Since heliostats are so costly with respect to other parts of the plant, they are an obvious candidate for scrutiny in trying to reduce system costs.

Changes in heliostat design, however, may lead to changes in heliostat performance, which, in turn, affect not only field size and layout, but also receiver size and tower height. Thus, the impact of the design change on other parts of the central receiver system, as well as on the heliostat itself, must be taken into account in evaluating the change.

This study provides results which can be used to identify cost effective modifications to the current baseline glass/metal heliostat design [2]. Specific design changes are not analyzed because it is often the case that any one or a combination of several changes can lead to the same change in heliostat performance. Instead, the results are generalized in terms of the heliostat breakeven cost; i.e., the cost of the "new" heliostat design as a function of heliostat performance required to give the same system energy cost as the baseline design. The breakeven cost reflects the total system cost/performance tradeoffs resulting from changes in the baseline heliostat design. The results can be used for evaluating proposed changes in a mass produced version of the baseline design, for re-evaluating current specifications (e.g., pointing accuracy and stow requirement) for all designs, and for assessing designs radically different from the baseline case.

Breakeven Cost Analysis

The breakeven cost is useful for quantifying the minimum savings which must be obtained in a new design which degrades performance (or conversely, the maximum allowable expenditure in the case of a performance improvement). Thus, design changes can be screened with respect to their potential effectiveness before a complete redesign is undertaken.

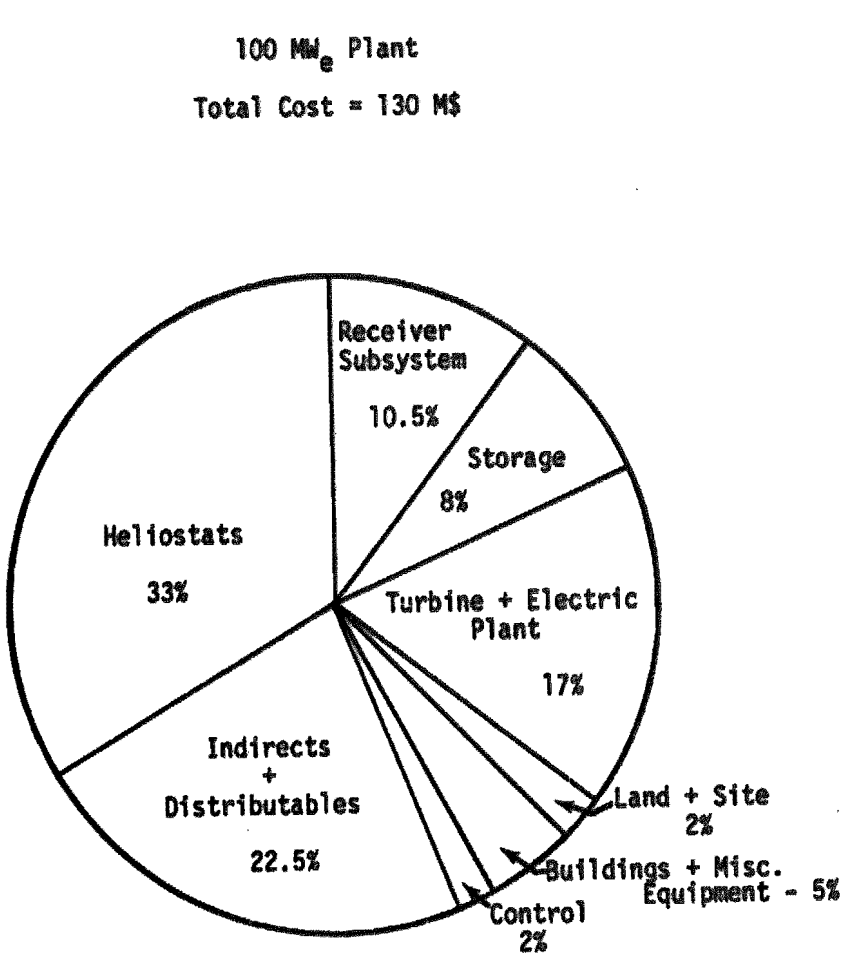

Figure 1. Capital Cost Breakdown for Advanced Sodium Receiver Design; Solar Multiple = 1.5 [1]

Because of the strong coupling of heliostat design to other system elements, particularly receiver size and tower height, each change in heliostat performance requires reoptimization of the system design. For example, consider the use of a cheaper, but less accurate tracking mechanism. Figure 2 illustrates the system tradeoffs which result. To obtain the same plant output, both a larger receiver with greater costs and losses, and more heliostats placed farther from the receiver are required. The resulting system design is that combination of field layout, receiver size, and tower height giving the lowest system energy cost.

The degree of leverage allowed by a particular type of design change will depend on the details of the heliostat being evaluated. However, a qualitative feel for interpreting the breakeven cost in view of high vs. low leverage options can be gained from Figure 3. Two sample curves of breakeven cost vs. tracking error are given. (These different curves can arise because of differences in the base case cost, as discussed in a later section.) Suppose the tradeoff calculations result in the curve labeled high leverage. Then the heliostat designer would probably have a wider variety of options for redesign since the high leverage case requires smaller cost savings for performance degradations than the low leverage case. In other words, the remainder of the system is not as sensitive to tracking error in the high leverage case.

The necessary system reoptimization when heliostat performance is changed plus the dependence of results on system size and base case cost have been calculated with the DELSOL code described in references 3 and 4. Details of the cost and performance models are found in the code manual [4].

Base Case and Assumptions

Specifications of the baseline heliostat and other system information are summarized in Table I. The heliostat is an advanced glass/metal design whose cost (excluding wiring) is consistent with a production rate of 25,000 units per year [5]. Heliostat field densities are based on the optimal spacings for the baseline case. Tracking and surface errors are assumed to have normal distributions. The system design, receiver performance, cost, and economic assumptions remain the same for all cases studied. Values for the relevant costs and non-field performance are found in reference 4.

In addition, both the heliostat and balance of plant operating and maintenance (O&M) charges were assumed the same as the base case for all other cases studied. A value of 1.5% of the direct capital cost was used as the first year base case heliostat charge, based on contractor estimates and washing studies [2,7]. (This value levelizes to 2.74% per year over the life of the plant, using the economic assumptions in the DELSOL code.) A 1.5% charge was also used for the balance of plant rate. When applying the results given below to a heliostat with a different O&M rate, the differences in O&M must be included in the breakeven cost. Only the differences are important since every case has been analyzed with the 1.5% first year charge of the base case. An example of applying these ideas is given below in the discussion on reflectivity.

EXAMPLE: CHEAPER TRACKING MECHANISM

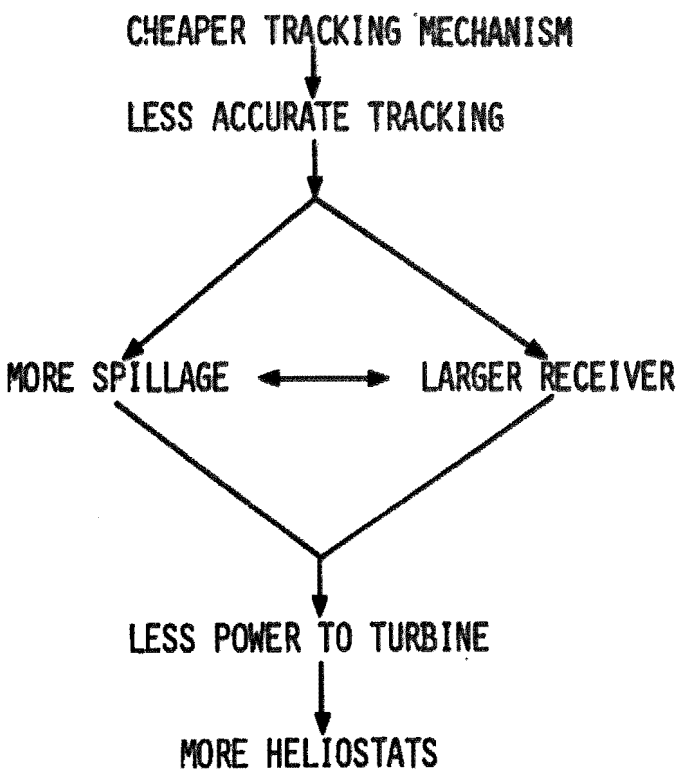

Figure 2. System Tradeoffs for Cheaper, Less Accurate Tracking

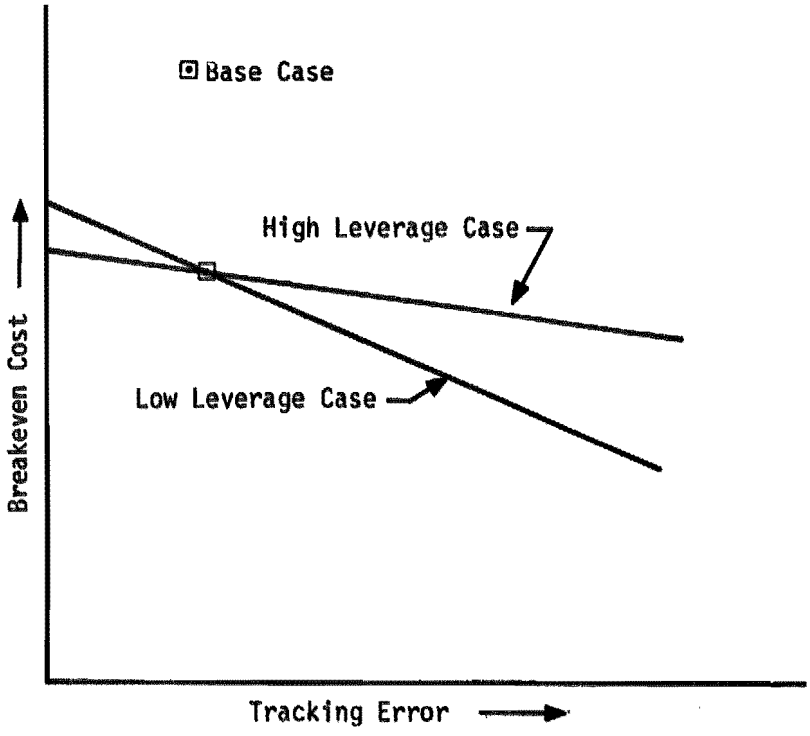

Figure 3. Illustration of High vs. Low Leverage Options

TABLE I

SUMMARY OF BASE CASE

Heliostat	
Square	7.4 m x 7.4 m
	89.7% reflective surface
Glass	0.89 reflectivity, average between washings
	1.0 mrad std. dev. in surface errors, each axis
AZ-EL Tracking	0.75 mrad std. dev. in gimbal axis errors, each axis
Canted	2 panels across, 6 down
	Single, on-axis cant and focus at 6 tower heights
Cost	$\$65/m^2$ (includes installation, but not wiring)
System	
Single module	
Solar multiple = 1.5*	
Receiver	
External cylindrical, advanced sodium [4]	
No flux limit**	
Costs	
Suggested by advanced sodium design [4]	
Heliostat O&M - optimum washing sequence [7]; contractor estimates on part replacement [2]	
Economics	
Capital escalation = 8%/yr	
General inflation = 8%/yr	
Cost of money = 10%/yr	
Operating life of plant = 30 yrs	
Fixed charge rate = 17.75%/yr	

*Changing the solar multiple affects breakeven cost in a similar manner to changing plant size. The "Results" section points out when this is important.
**The imposition of a flux limit has little effect on the value of the breakeven costs.

The heliostat design variables analyzed are mirror reflectivity, beam pointing accuracy, surface quality, canting and focusing strategy, heliostat size, and stow requirements. Some of the interactions when two or more design variables are changed simultaneously are also discussed. Finally, changes in the baseline heliostat cost are considered.

The results are applicable both to changes in subcomponents of the baseline design and to evaluation of designs completely different from the baseline heliostat. Examples of each type are given in the discussion below. Both $\$/m^2$ and $\$/m^2/yr$ are presented. The former value represents the capital cost plus present worth value of the difference in O&M between the new design and the baseline heliostat. The latter is the annualized capital cost plus the levelized value of the annual O&M cost difference between the two designs. (See the Appendix for the relation between these two scales.)

Results

Reflectivity. The reflectivity dependence of the breakeven cost is given in Figure 4. The time averaged value of the reflectivity between washings is used here. Three curves are drawn: the result for a 25 MW_e plant, that for a 300 MW_e plant, and the current cost goal for heliostats recommended to DOE. The curves for the two plant sizes indicate first, that the breakeven cost is strongly dependent on reflectivity and second, that system size dependence becomes more pronounced the lower the reflectivity. Two compounding effects are folded into this latter result. First, at a given reflectivity, the larger the plant size (i.e., field size), the poorer the field performance since heliostats are placed in the larger system at positions with greater attenuation (north field) or poorer cosine (south field). Second, for a given plant size, a decrease in reflectivity means a greater number of heliostats. Again, these heliostats must be placed at locations of poorer performance. The combination of these two effects leads to the divergence of the curves observed in Figure 4.

The current recommended cost goal for heliostats is $\$72/m^2$*reflectivity. However, Figure 4 indicates that low reflectivity heliostats meeting the goal would in fact be too expensive in comparison with the base case design. The goal came from the first order consideration that the number of heliostats is inversely proportional to the reflectivity for a given size system. However, it does not include the effect that the larger field size required with lower reflectivity heliostats is poorer performing as described above. Hence, a greater than proportional number of heliostats is required as reflectivity drops.

The reflectivity results provide a useful example for evaluating a design concept which differs dramatically from the baseline heliostat. This example illustrates the necessity of accounting for O&M differences between designs. One of the current designs is a low reflectivity (0.6) unit covered with an inflated plastic dome [6]. The breakeven cost in Figure 4 for this design is $\$38.50 - \$35/m^2$ ($\$8.20 - \$7.40/m^2/yr$) in the range of 25 - 300 MW_e. Remembering, however, that the calculations are based on the same O&M rates

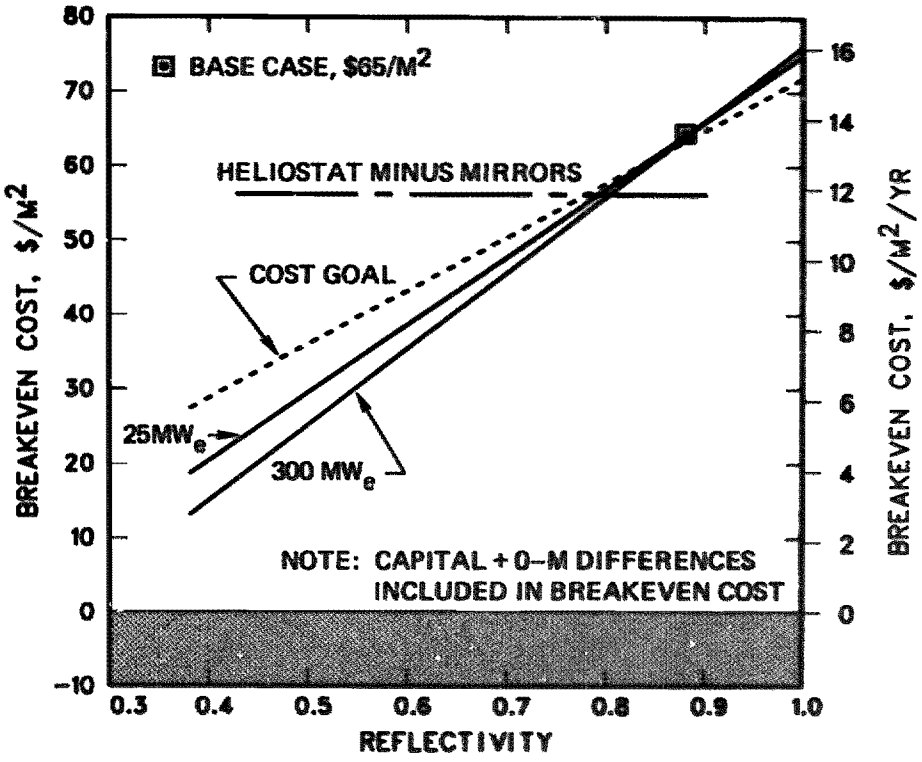

Figure 4. Heliostat Breakeven Cost Vs. Mirror Reflectivity; Base Case, $65/m^2

among designs, we must take into account any differences in O&M between the baseline and actual design being evaluated. In fact, because of the plastic dome, this design does have a higher O&M charge. Using the economic scenario assumed in this study and including two dome replacements during the 30 year plant life, the additional present worth of O&M based on an optimal washing sequence for this design is ~$15.70/m^2 ($4.95/m^2/yr) [6,7]. The breakeven capital cost then becomes $22.80 - $19.30/m^2 in the 25 - 300 MW_e range.

Another useful result is presented in Figure 4. Suppose one were considering simply the substitution of a different reflective surface in the baseline design. The dashed line labeled "Heliostat minus Mirrors" is the cost of the total baseline unit less the cost of the reflective surface. In other words, there will be $56/m^2 cost regardless of what reflective surface is used. We see that this line intersects the breakeven cost curves at ~0.8 reflectivity. This means that if the time averaged reflectivity of the substitute surface is below 0.8, then the total unit must cost less than $56/m^2 to give the same system energy cost, or the cost of the reflective surface must be negative. Put another way, any surface of average reflectivity below 0.8 could not lead to the same system energy costs even if it were free.

The importance of system redesign as heliostat performance is changed is illustrated in Table II. The optimal tower height and receiver diameter are given for the 25 MW_e and 300 MW_e plants. In both cases the larger field sizes required as reflectivity drops lead to higher towers and/or larger receivers.

TABLE II

OPTIMAL TOWER HEIGHT AND RECEIVER SIZE FOR VARYING REFLECTIVITY

Reflectivity	25 MW_e Tower ht. (m)*	25 MW_e Rec. diam. (m)**	300 MW_e Tower ht. (m)*	300 MW_e Rec. diam. (m)**
1.0	100	8	280	20
Baseline (0.89)	100	8	280	22
0.8	100	8	300	22
0.7	100	8	320	24
0.6	120	8	360	26
0.5	120	8	400	28
0.4	140	10	400	28

*DELSOL considers only discrete values of the tower height and receiver size.
**External cylindrical receivers, height = diameter.

Pointing Accuracy. In the azimuth-elevation tracking scheme of the baseline design, the pointing accuracy of the heliostat is characterized by separate errors in the azimuthal and elevation drive directions. Sources

common to both types of errors include tower sway (on which heliostat design has no effect), heliostat misalignment (i.e., miscalibration of the set point for the control schemes), and both plastic and elastic deformations of the foundation, structure, and/or pedestal due to wind and gravity loads. Periodic recalibration can eliminate heliostat misalignment errors, and the structural design minimizes deformations by wind and gravity. The motor and drive mechanism of the respective tracking direction is a unique source for each error.

Figure 5 gives the breakeven cost for the total heliostat unit (upper curve) and for the azimuthal tracking subcomponent (lower curve) as a function of the standard deviation of the azimuthal tracking error. The dependence on plant size is 5% or less between 25 and 300 MW_e; the results here are for an intermediate 100 MW_e size.

The breakeven cost for the total heliostat unit in Figure 5 is useful for evaluating designs considerably different from the baseline in which a number of factors combine to produce a different tracking accuracy. Suppose, for example, that a new design has a different azimuthal tracking scheme and lighter structural support. These might combine to give an estimated error of 4 mrad in the new design. From Figure 5, the new design must cost less than ~\$59/m^2 (\$12.50/m^2/yr), including any difference in operating and maintenance between the two designs, in order to be cost effective. Equivalently, the total savings in the new design must be greater than the base case minus the breakeven cost at 4 mrad, or greater than \$6/m^2 (\$1.30/m^2/yr).

The breakeven cost for the azimuthal drive subcomponent is simply the upper curve minus the baseline cost excluding the drive and motor [2]. As with the "Heliostat minus Mirrors" line of Figure 4, this result is useful for evaluating different drive designs in the baseline heliostat, as opposed to completely different total heliostat designs considered in the previous paragraph. In Figure 5, we see that the breakeven cost is positive only if the azimuthal error is less than ~4.0 mrad. In other words, inaccuracies greater than 4 mrad will always yield a greater system energy cost even if the drive mechanism is free. At the other extreme of zero azimuthal tracking error, the new drive must cost practically the same as the baseline component. In this case, little is to be gained in the system from greater accuracy because reflected image sizes are dominated by heliostat size, sunshape, and/or surface errors.

The results in Figure 5 reflect not only different field sizes resulting from changes in heliostat performance, but also different costs and performance in other parts of the system as well. Figure 6 illustrates the performance trades made between the field and receiver design as the azimuthal tracking accuracy decreases. All performance results correspond to an optimally designed 100 MW_e system. Only the radiation/convection and intercept factors vary significantly. With larger errors leading to larger reflected images, a larger receiver is required to intercept the flux. However, the penalty of a larger receiver is increased radiation and convection losses. The cost effective result is a trade of greater spillage for reduced receiver losses and receiver costs.

Figure 7 is the result for inaccuracies in the elevation tracking direction. The curves and their interpretation are similar to the azimuthal

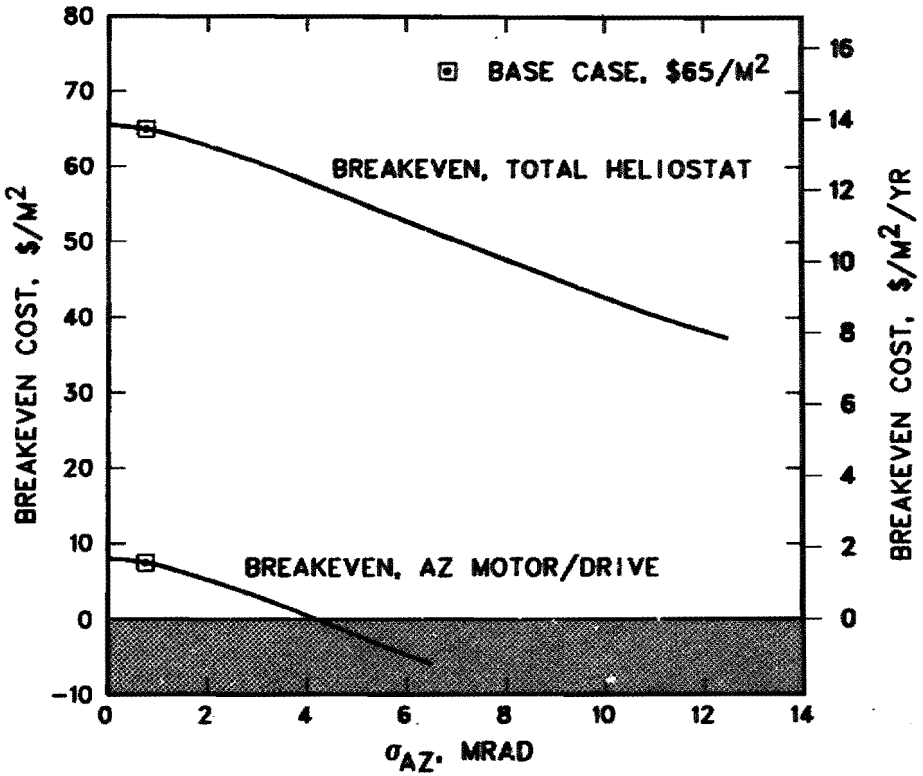

Figure 5. Heliostat Breakeven Cost Vs. Azimuthal Tracking Error; Base Case, $65/m2

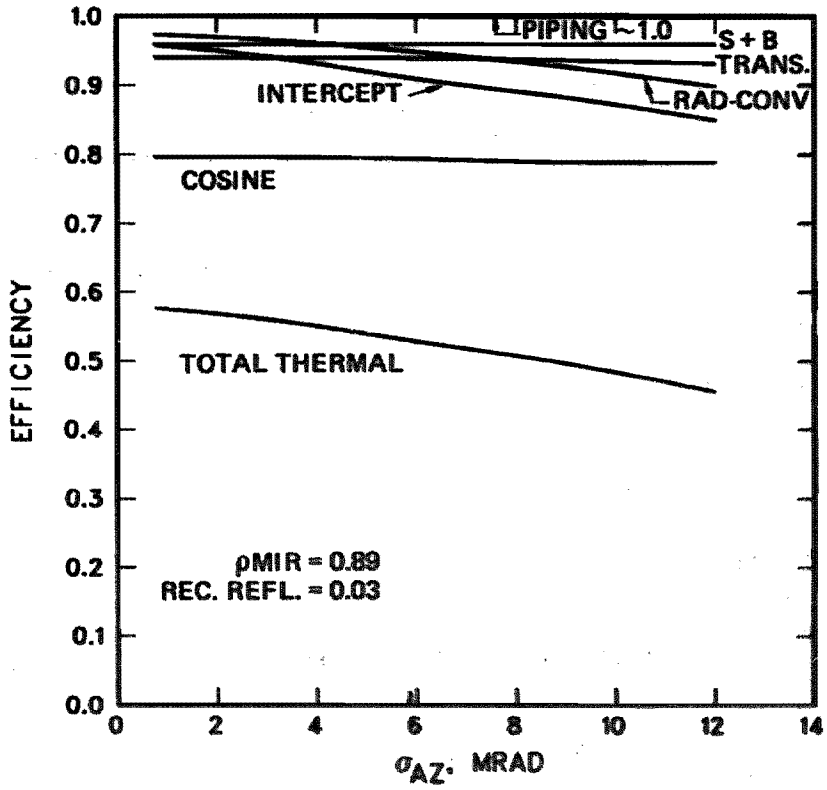

Figure 6. System Thermal Performance Vs. Azimuthal Tracking Error; 100 MW_e Plant

Abbreviations:
- S + B = shadowing and blocking
- TRANS. = atmospheric transmissivity
- RAD-CONV = receiver efficiency (1 - radiation/convection loss)
- ρMIR = mirror reflectivity
- REC. REFL. = receiver reflectivity

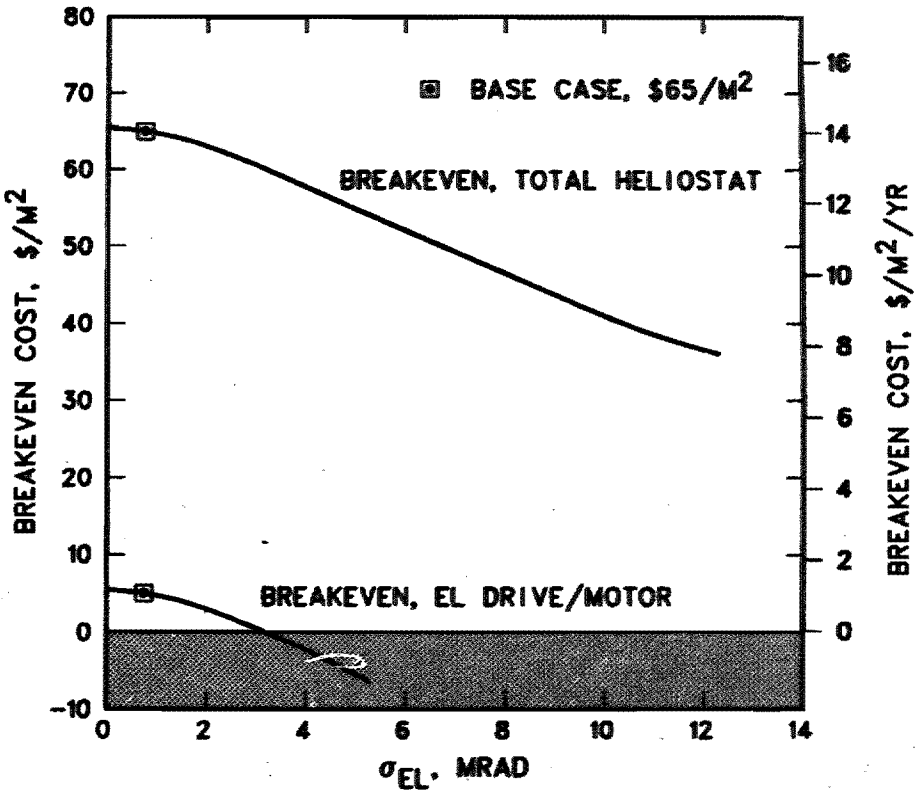

Figure 7. Heliostat Breakeven Cost Vs. Elevation Tracking Error; Base Case, $65/m2

tracking error case of Figure 5. In this instance, the elevation tracking subcomponent is a smaller part of the total cost (lower curve) so that a limit of only ~3 mrad in the elevation tracking accuracy in the baseline design can be tolerated for the same system energy costs.

Surface Quality and Alignment. The mirror surface is generally defined so that "x" indicates the direction parallel to the ground when the mirror is vertical, and "y" is vertical to the ground, perpendicular to x. Sources for errors in either the x or y mirror direction include surface waviness, non-specularity, glass deformation with temperature, and misalignment of the mirror panels with respect to the canting specification for the design.

Figures 8 and 9 present results for surface errors in the x surface direction (standard deviation σ_{sx}), and both the x and y directions (σ_{sx} and σ_{sy}), respectively. The σ_{sy} curve is practically the same as the σ_{EL} result in Figure 7, and is not presented here. As with the tracking errors, the dependence on plant size is small, and only the 100 MW_e curves are given.

The interpretation of the curves is similar to the analysis of the tracking errors. The upper curve in each figure is useful for comparing completely different designs, while the lower curves offer examples for evaluating options in subcomponent design. For example, suppose that mirror waviness is the primary cause of surface errors in the longer panel dimension (x in the baseline design). The lower curve in Figure 8 is the result for the mirrors panels only. It indicates that the limit for poorer quality mirrors would be ~4 mrad error at zero cost. Similarly, we obtain the lower curve in Figure 9 by assuming that the backing structure is the mainstay for panel alignment and that it contributes equally to both surface errors.

It is worth noting that the breakeven costs in the σ_{sx} case are less than the analogous σ_{AZ} values as the errors increase above the base case values (and correspondingly, greater below the base case values). The reason is that random surface error effects are independent of field position while azimuthal tracking inaccuracies become unimportant in that part of the field in line between the sun and receiver. Hence, in a time averaged result, as this one is, azimuthal errors will produce smaller penalties at larger errors (and also smaller potential savings at smaller errors) than horizontal slope errors of the same magnitude.

Canting and Focusing. Focusing reduces the size of the image reflected from a heliostat, allowing a smaller receiver size with reduced costs and losses. From a performance viewpoint, it would be best to focus individually each heliostat with respect to its position in the field. However, the economics of mass production will probably limit heliostats to only one or a small number of focal lengths. In addition, instead of the continuous bend in the reflective surface required for focusing, it may be cheaper to approximate the curvature by a number of smaller tilted flat panels. This latter option is called canting.

Table III offers the results for several canting/focusing strategies. The base case is a canted design with a single focal length for the field; in

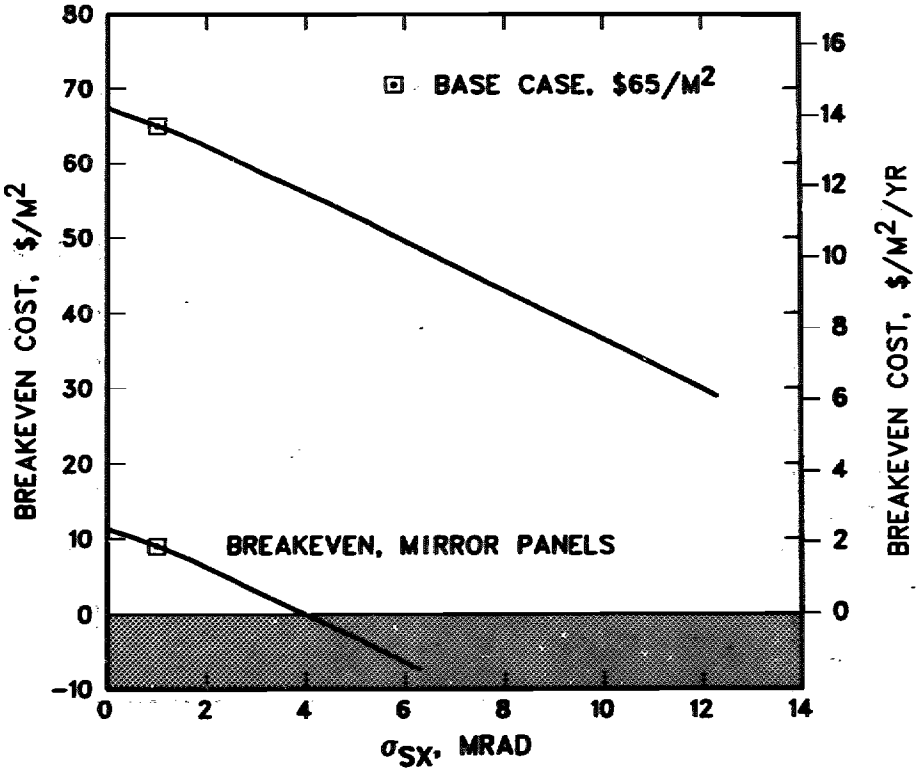

Figure 8. Heliostat Breakeven Cost Vs. Horizontal Surface Error; Base Case, $65/m^2

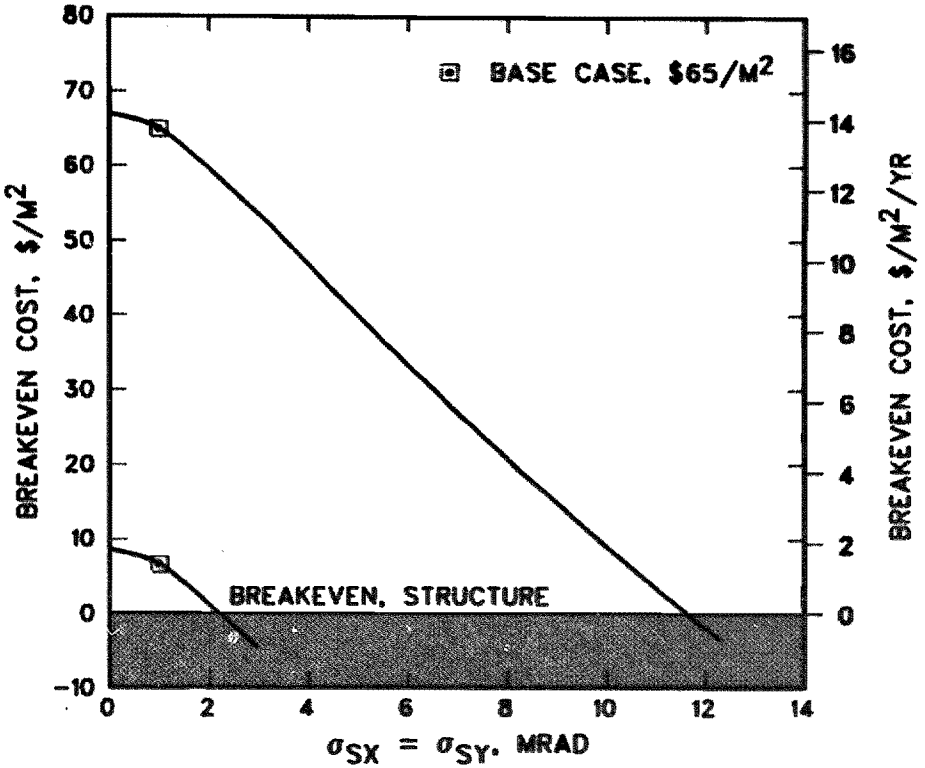

Figure 9. Heliostat Breakeven Cost Vs. Equal Surface Errors: Base Case, $65/m^2$

addition, each mirror panel is curved in the longer panel dimension to the same focal length. The results are as expected. Individual focusing should be and is the best option, but it is only slightly better than individual canting. Note that the effects are more pronounced in the smaller system where heliostat size is more influential in the system design. In the larger systems, all options approach the base case so that individual focusing or canting is not worth much in a larger system application.

TABLE III

BREAKEVEN COSTS FOR VARIOUS CANTING AND FOCUSING OPTIONS

Design	Breakeven Cost ($/m^2)		
	25 MW_e	100 MW_e	300 MW_e
Individual focus, every heliostat	69.50	65.50	65
Individual cant, every heliostat, single focus, all panels	68.10	65.40	65
Single focus, all heliostats (no cant panels, single curved surface)	66.20	65.10	65
Baseline: single cant, all heliostats; single focus, all panels	65	65	65
Flat, no canting or focusing	56.50	62.40	63.80

Size. The question of optimal heliostat size is based on the cost/performance tradeoff which favors, on the one hand, larger sizes to take advantage of economies of scale, and on the other, negligibly small sizes to eliminate the contribution of heliostat size to reflected image sizes. Since mass production will tend to limit heliostats to one size, the identification of a reasonable size for a range of applications, if possible, becomes a worthwhile endeavor.

Figure 10 is the plot of the influence of individual heliostat size on breakeven cost. The 25, 100, and 300 MW_e plant sizes are included. Field wiring costs have been excluded in order to avoid uncertainties related to the scaling of wiring costs with heliostat size. (Note: A realistic scaling should produce larger relative wiring costs per heliostat as the size decreases. This would lead to a downturn of the curves instead of the leveling out observed at smaller sizes in Figure 10.)

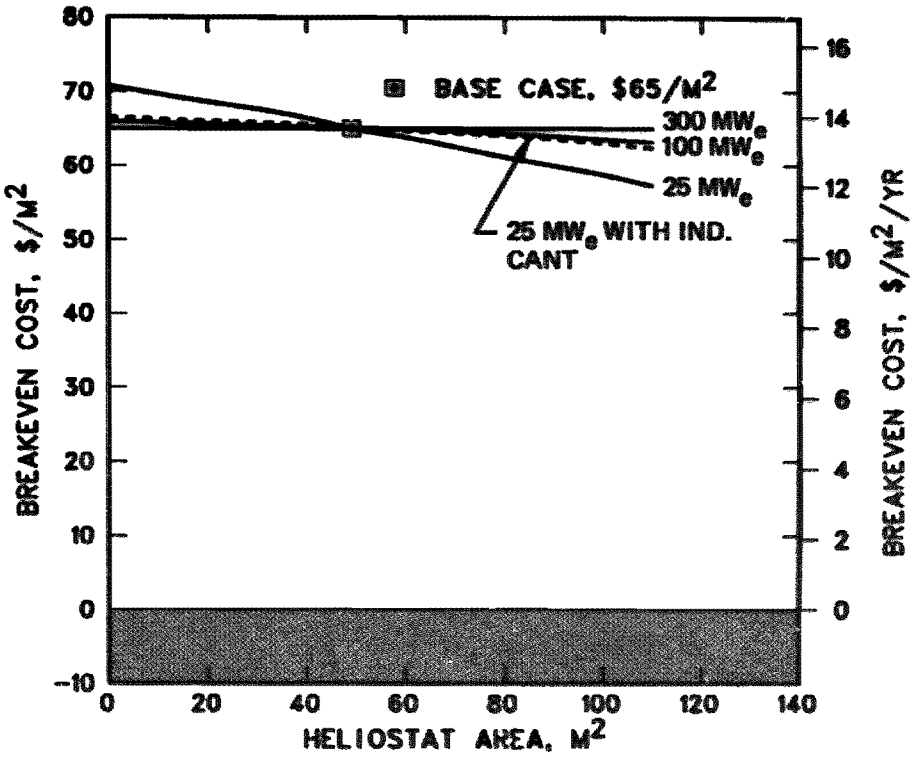

Figure 10. Heliostat Breakeven Cost Vs. Heliostat Size, Base Case, $65/m^2

Individual heliostat size has very little influence in the larger plants where sunshape and errors dominate the reflected image sizes in the spillage/receiver loss trade. It becomes more significant in smaller systems where the field sizes are small enough for heliostat size to contribute to image sizes. The effect can be minimized if the heliostats are individually canted. The breakeven cost for a 25 MW_e system with an individually canted heliostat is given by the dashed line in Figure 10, which is practically coincident with the 100 MW_e result.

In all cases the curves eventually level out in going to smaller sizes. The "small enough" value depends on the system size; this analysis indicates ~5 m^2 vs. 75 m^2 for the 25 vs. 300 MW_e plants. Below these values sunshape and errors dictate image sizes and hence, the trade between spillage and receiver losses in an optimally designed system. In other words, for heliostats sized in the plateau region of the curve for a given plant size, the same receiver size and tower height would be selected in an optimal design.

At the other end of larger sizes, one can always find a heliostat large enough for the given system which will still influence image sizes, and hence the optimal choice of receiver size, tower height, and field layout.

Overall, the results indicate that practical economies of scale should be taken advantage of, particularly if individual canting or something approaching it can be cheaply implemented for small scale applications.

Stow Requirement. In the base case design, 89.7% of the overall area is reflective surface. The other ~10% is primarily a slot down the center between the two rows of panels to allow for inverted stow of the heliostat in the case of hail and high winds. Proposals have been made to eliminate the stow requirement and extend the mirror panels to fill the slot. In the limit of complete mirror coverage in the base design, the justifiable breakeven cost becomes ~\$67.50/m^2 (\$14.35/m^2/yr), independent of system size. From the cost breakdown for the base design [2], the expense of the added glass and structure less the savings from eliminating the stowing motor and jack amounts to a net savings of ~\$4/m^2, or a total capital expense per heliostat of \$61/m^2. Additional O&M for extra washing and glass replacement due to hail damage may be necessary in this modified design. However, if its present worth value is less than the \$6.50/m^2 (levelized yearly cost of \$1.40/m^2/yr) margin indicated here, then such a design change would be justified.

Interactions. Figure 11 is an example of the results obtained when two design variables are changed simultaneously. In this case, the azimuthal and elevation tracking errors are both varied. The solid line is the actual result while the dashed line represents the additive result from Figures 5 and 7. A small synergistic effect can be seen. With the two errors degrading simultaneously, both a larger, less efficient receiver and additional heliostats at poorer locations are required in comparison with the case in which only one error is varied at a time.

In other combined cases analyzed, the magnitude of the interactions is usually small, as in the az-el case, so that the result of combined changes can be roughly approximated by looking at each change in turn. (A reminder

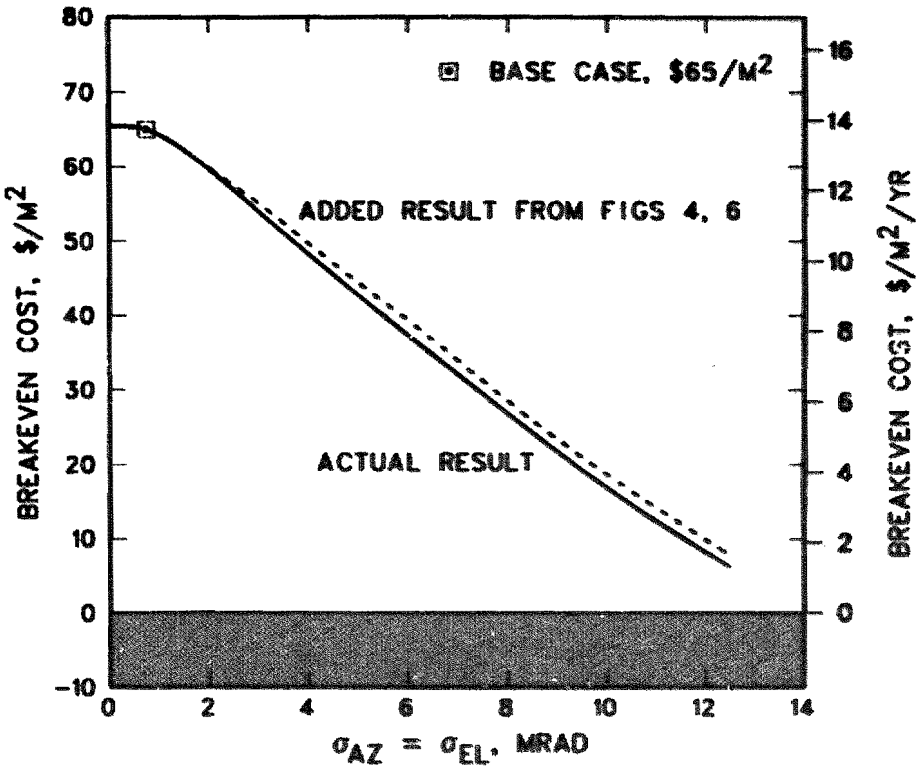

Figure 11. Heliostat Breakeven Cost Vs. Equal Az-El Errors; Base Case, $65/m^2

in carrying out such an exercise for combined error analyses: when errors act in the same direction, e.g., azimuthal tracking and surface errors in the x-direction, the combined error is the square root of the sum of squares of the individual errors.)

It is generally true that design changes which simultaneously degrade several aspects of heliostat performance do result in breakeven costs less than those considering each change sequentially. However, when certain performance characteristics are improved while others are degraded, the magnitude and direction cannot be generally predicted.

Changes in the Base Case Cost. The $\$65/m^2$ cost for the baseline design is the goal for a mass produced version which might allow large central receiver solar plants to become competitive in a wide range of electrical and process heat markets. At this point, costs are a considerable way from meeting the goal; current estimates lie between $\$275/m^2$ and $\$325/m^2$ for the Barstow pilot plant units. In order to evaluate current design and design modifications during these early stages of development, additional curves are presented in Figures 12-15 for varying base case costs of $\$250/m^2$, $\$150/m^2$, and $\$100/m^2$; results for an optimistic $\$40/m^2$ are also included. For conciseness, the curves are normalized to the base case cost. Reflectivity, azimuth and elevation errors, and surface errors in the x-direction (y-direction is quantitatively the same as the elevation error case) are reevaluated. The other design aspects discussed for $\$65/m^2$ have not been included since the impact of such changes on the breakeven cost is not usually large. When considering simultaneous design changes to the baseline, an approximation can be obtained by looking at each change in turn, remembering the caveats discussed above in the section on interactions.

For a base case cost intermediate between the results given here, the breakeven cost can be estimated by interpolating on the percent change in the breakeven cost between the two appropriate results. For example, suppose we want to evaluate a degradation in reflectivity to 0.7 in a baseline design costing $\$200/m^2$. The percent change at $\$250/m^2$ is ~25%, and at $\$150/m^2$, ~33% (Figure 12b, 300 MW_e size). Interpolating gives a 29% change for $\$200/m^2$, or a breakeven cost of $\$142/m^2$ ($\$30.20/m^2/yr$). (Note that a visual interpolation would suffice in most cases since successive curves lie close together.)

It is generally true that as the base case cost goes down, the percent change in breakeven cost with respect to the baseline cost for a given design change becomes larger. It happens that as the heliostats become cheaper relative to the associated land and wiring costs, the optimal field layout, based on the field cost/performance ratio, is shifted toward the southern part of the field. The shorter wiring runs and greater heliostat densities begin to compensate for the poorer performance in the more southerly areas. In addition, the receiver and tower represent a larger proportional cost as heliostat cost decreases, so that the most cost effective designs tend toward smaller receivers and/or shorter towers at the sacrifice of greater spillage. Thus, the overall field performance of the optimally designed system decreases as the cost of heliostats goes down. As a result, degradations in heliostat performance lead to greater relative changes in breakeven costs to make up for the field performance decline accompanying the layout of cheaper heliostats. (Keep in mind that while the percent change in breakeven cost may be greater as the base case cost decreases, the actual $\$/m^2$ change will be less.)

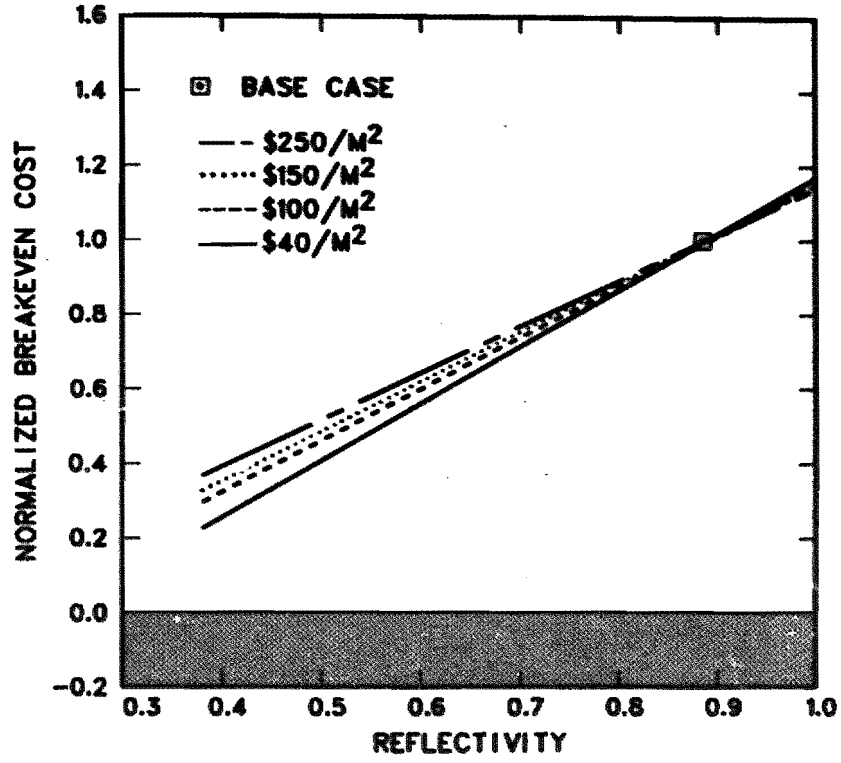

Figure 12a. Normalized Breakeven Cost Vs. Mirror Reflectivity; 25 MW_e Plant

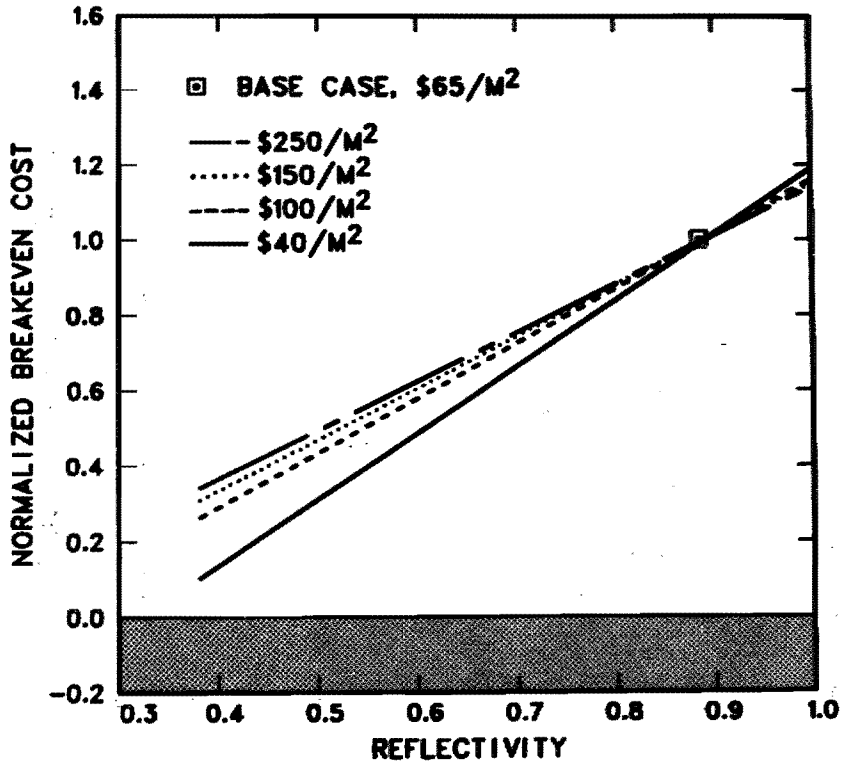

Figure 12b. Normalized Breakeven Cost Vs. Mirror Reflectivity; 300 MW_e Plant

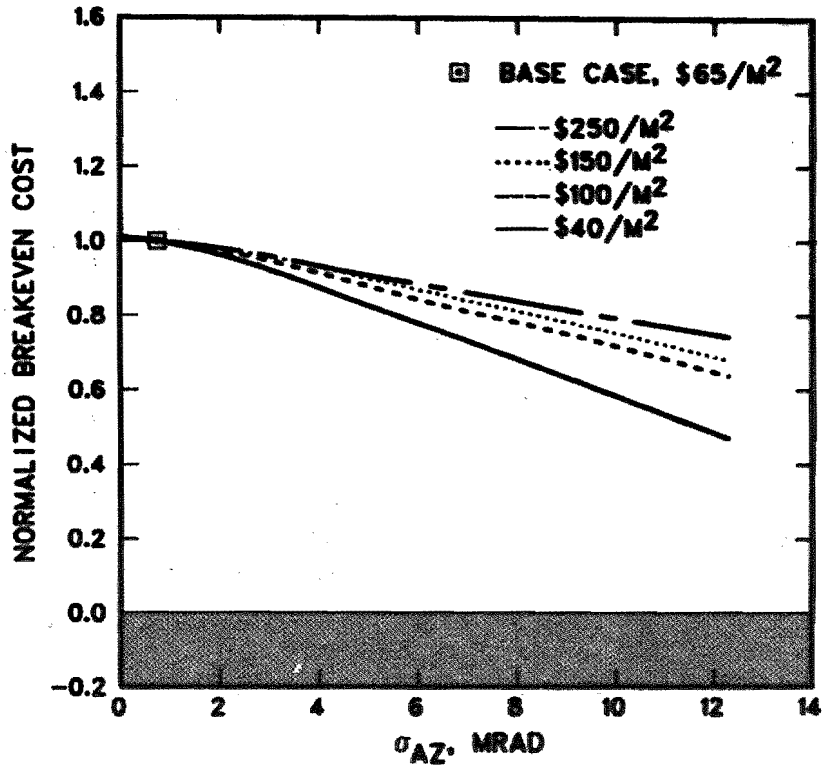

Figure 13. Normalized Breakeven Cost Vs. Azimuthal Tracking Error

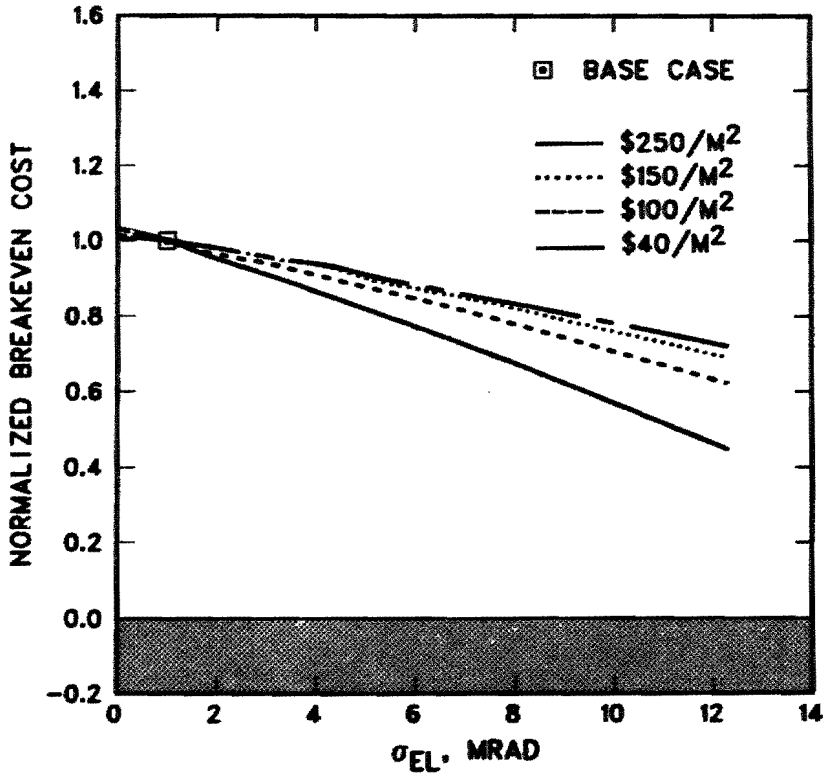

Figure 14. Normalized Breakeven Cost Vs. Elevation Tracking Error

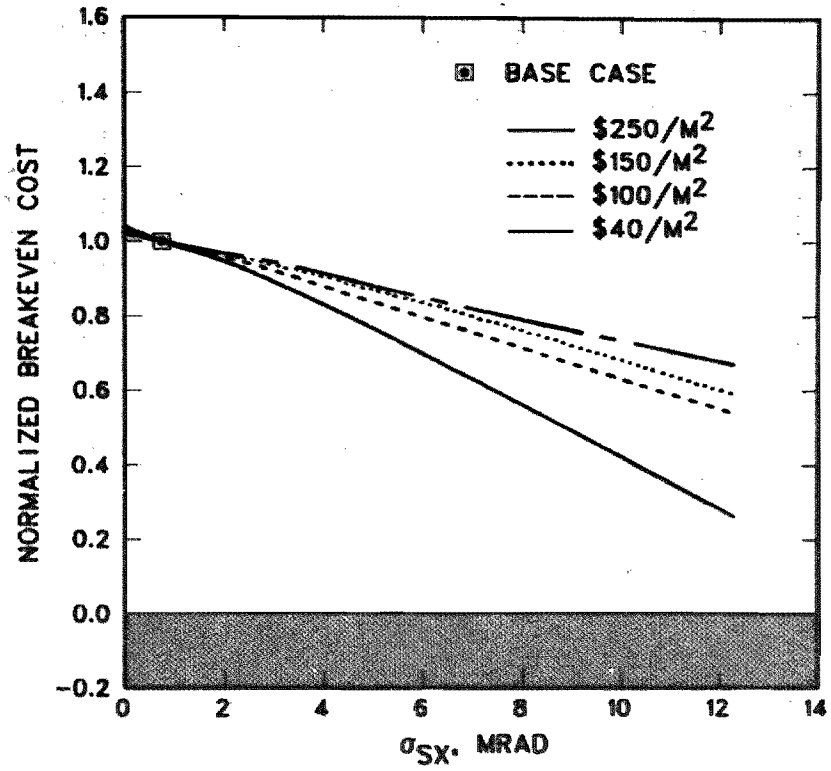

Figure 15. Normalized Breakeven Cost Vs. Horizontal Surface Error

How to Use the Results

The application of the results has been illustrated with several examples throughout the text. Both changes in subcomponents and totally different designs can be evaluated. In summary the results should be used as follows:

1. Identify attractive new designs or promising changes in the baseline design.

2. Determine the actual cost and corresponding change in heliostat performance. Differences in O&M must be included here. This value can be on a $\$/m^2$ basis (capital cost + present worth of additional O&M), or on a $\$/m^2/yr$ basis (annualized capital cost + levelized additional O&M).

3. Use Figures 4-15 to find or estimate the breakeven cost. These results correspond to systems optimally designed for the new heliostat. If the comparison is in $\$/m^2/yr$, care must be taken either to use the same economic scenario described in Table I, or to adjust the right hand scale according to equation (3) in the Appendix.

4. If the new cost is less than the breakeven cost, then the new design is justified.

Conclusions

The results presented here have been used to suggest bounds on the changes in performance which could be tolerated in the base case design. Because no single component dominates the total cost of the base design, the margins for less accurate tracking, poorer quality mirrors, etc. are small in the absolute sense. However, relative to the base case, we might consider changes which degrade the performance by a factor of 2-3 (e.g., a cheaper tracking drive) if the changes could be implemented cheaply enough. In other words, a more cost effective design could result from several small modifications rather than one major one.

The results can also be applied to radically different design concepts which might cost considerably less at the sacrifice of some performance parameter, as, e.g., reflectivity in the plastic dome designs. The results can then be used as a guide to the cost effectiveness of a new design, provided differences in O&M are accounted for.

Of the design changes considered, reflectivity, tracking accuracy, and surface quality and alignment show the greatest changes in breakeven cost over the ranges of these variables analyzed. In larger systems (100 MW_e or bigger), cost effective heliostat designs are practically insensitive to the size and canting and/or focusing strategy selected. As system size decreases, however, these parameters become more important. Their effect in plant sizes less than 25 MW_e remains to be determined. Finally, it appears that the stow requirement in the baseline design might be profitably eliminated when the added O&M for more glass area to wash and replace is taken into account.

REFERENCES

[1] Usborne, D. and Tallerico, L., private communication (Sandia revised costs for 100 MW_e advanced central receiver designs), February, 1979.

[2] McDonnell Douglas Astronautics Co., "Solar Central Receiver Prototype Heliostat CDRL, Final Technical Report," Rpt No. MDC-G7399, Item B.d, August, 1978.

[3] Dellin, T. A. and Fish, M. J., "DELSOL: A Code for Central Receiver Performance and Optimization Calculations," presented at the International Solar Energy Society meeting, Georgia, May, 1979.

[4] Dellin, T. A. and Fish, M. J., "A User's Manual for DELSOL: A Computer Code for Calculating the Optical Performance, Field Layout, and Optimal System Design for Solar Central Receiver Plants," SAND79-8215, Sandia Laboratories, June, 1979.

[5] Eason, E. D., private communication, April 1979.

[6] General Electric Energy Systems Program Department, "Solar Central Receiver Prototype Heliostat Phase I, Final Technical Report," Rpt. No. SAN-1468-1, October, 1978.

[7] Eason, E. D., "The Cost and Value of Washing Heliostats," presented at the International Solar Energy Society meeting, Atlanta, Georgia, May, 1979.

APPENDIX--EQUATIONS FOR THE BREAKEVEN COST

The breakeven heliostat cost is calculated to yield the same levelized busbar energy cost as the base case system. The busbar energy cost is calculated from the following simplified formula:

$$BBEC = \frac{(FCR \times CC_{TOT}) + (\overline{OM}_H \times CC_H) + (\overline{OM}_{BOP} \times CC_{BOP})}{kw\text{-}hr_{NET}} \qquad (1)$$

where

$BBEC$ = busbar energy cost ($/kw-hr);

FCR = fixed charge rate;

CC_{TOT} = total capital cost of the plant;

$\overline{OM}_H$ = levelized yearly operating and maintenance rate for the heliostats, expressed as a fraction of the heliostat capital cost;

CC_H = heliostat capital costs;

$\overline{OM}_{BOP}$ = levelized yearly operating and maintenance rate for the balance of plant (non-heliostat), expressed as a fraction of the balance of plant capital costs;

CC_{BOP} = balance of plant capital costs;

$kw\text{-}hr_{NET}$ = net yearly energy production by the plant.

Writing equation (1) first for a baseline heliostat design and then for some other design, and setting the two equations equal, one can find the allowed total expenditure for heliostat with the second design to give the same system energy cost as with the baseline design. Denoting base case values with superscript B, and the values with the new design N, the breakeven cost in $\$/m^2$ is given by:

$$BEC_H(\$/m^2) = \left\{ \frac{kw\text{-}hr_{NET}^{N}}{kw\text{-}hr_{NET}^{B}} \quad \frac{FCR + \overline{OM}_H^B}{FCR + \overline{OM}_H^N} \times \left[\frac{FCR + \overline{OM}_{BOP}^B}{FCR + \overline{OM}_H^B} \left(CC_{BOP}^B - \frac{kw\text{-}hr_{NET}^{B}}{kw\text{-}hr_{NET}^{N}} CC_{BOP}^N \right) + CC_H^B \right] \right\} \Big/ NHEL/AMIR \qquad (2)$$

where NHEL = number of heliostats in the system with the new design;

AMIR = mirror area per heliostat.

Equation (2) is based on the assumption that $\overline{OM}_{BOP}^B = \overline{OM}_{BOP}^N$.
Expressed as $\$/m^2/yr$,

$$BEC_H(\$/m^2/yr) = (FCR + \overline{OM}_H^N)\ BEC_H\ (\$/m^2) \qquad (3)$$

UNLIMITED RELEASE

INITIAL DISTRIBUTION

Dr. J. D. Heidt
Dornier System
Postfach 1360
7990 Friedrichschafen
W. GERMANY

Tadayoshi Tanaka
Electrotechnical Laboratory
Energy Div., Energy Systems Section
5-4-1 Mukodai, Tanashi
Tokyo
JAPAN

Jean Verraver
Belgonucleaire
25, Rue du Champ de Mars
B-1050 Brussels
BELGIUM

Dr. Wolfgang Bulang
MAN-Neue Technologie, Abt. ENT/V6
Postfach 500620
8000 Munich 50
W. GERMANY

Prof. J. L. Abatut
LAAS
7 Avenue du Colonial Roche
31400 Toulouse
FRANCE

Claudio Arano
Centro Estudios Energia
Augustin de Foxa 29
Madrid
SPAIN

Dr. A. F. Baker
Beethoven allee 79- Corner
Vikloria Strasse
53 Bonn 2
W. GERMANY

Fernando Delgado
Empresa Nacional de Ingenieria
Centro Operativo Energia
Padilla
17 Madrid 6
SPAIN

Dr. Claude Etievant
CNRS/EDF Project Them
Direction des Estudes et Recheres EDE
8 Quai Watier
78 Chateau
FRANCE

DFVLR
5 Koln 90, Linder Hohe
Postfach 90 60 58
Cologne
W. GERMANY
Attn: Dr. Phil. H. Hertlein
Wilfred D. Grasse

Jose Hidalgo
CASA - Space Division
Rey Francisco 4
Madrid
SPAIN

Carlos Ortiz
INITEC
Padilla 17
Madrid
SPAIN

Central Mortgage and Housing Corp.
Ottawa K1A OP7
CANADA
Attn: John Wadsworth
Peter Russell

Dr. Hans J. Sternfeld
DFVLR
D-7101 Lampoldshausen
W. GERMANY

Dr. Phil. Jochen Hofmann
MBB, Space Div.
P. O. Box 1169
8000 Munich 80
W. GERMANY

Dr. Giovanni Germano
Snamprogetti
20097 S. Donato
Milan
ITALY

Sidonio de Fretas Branco Paes
Rua D. Pedro V, 53, 5
Lisbon 2
PORTUGAL

Dr. Friedrich Boese
INTERATOM
Friedrich - Ebert Strasse
D-5060 Bergisch Gladbach-Bensberg
W. GERMANY

Solar Energy Group, Center of Energy Studies
Indian Inst. of Technology, Delhi
New Delhi-110029
INDIA
Attn: Ashok K. Seth
H. P. Garg

Prof. Ugo Tarinelli
Comitato Nazionale per L'Energia Nucleare
Dipartimento Ricera Tecnologica de Base Avanzata
00100 Rome
ITALY

Booz, Allen, & Hamilton, Inc.
8801 E. Pleasant Valley Rd.
Cleveland, OH 44131
Attn: C. G. Howard

Scientific Applications, Inc.
1546 Cole Blvd.
Suite 210
Golden, CO 80401
Attn: Milt Hetrick

Scientific Applications, Inc.
18872 Bardini Ave.
Irvine, CA 92715
Attn: R. J. Hoffman

Solaramics, Inc.
1301 El Segundo Blvd.
El Segundo, CA 90245
Attn: H. E. Felix

General Electric
1 River Road
Schenectady, NY 12345
Attn: Richard Horton
Stuart Schwartz
John Garate
James Elsner

FMC
328 Brokaw Rd.
Santa Clara, CA 95052
Attn: Daniel DiCanio

Burns & Roe, Inc.
185 Crossways Park Dr.
Woodbury, NY 11797
Attn: Dr. Wann-Joe Sun

Stanford Research Institute
Menlo Park, CA 94025
Attn: Chandrakant Bhumralkar

Dynatherm Corp.
1 Industry Lane
Cockeysville, MA 21030
Attn: W. B. Bienert

Busche Energy Systems
7288 Murdy Circle
Huntington Beach, CA 92647
Attn: Ken Busche

A. M. Clausing
University of Illinois
266 Mech. Eng. Bldg.
Urbana, Illinois 61801

Brookhaven National Laboratory
Upton, NY 11973
Attn: G. Cottingham

Aerospace Corp.
El Segundo Blvd.
El Segundo, CA 90274
Attn: Philip de Rienzo

McDonnell Douglas
5301 Bolsa Ave.
Huntington Beach, CA 92647
Attn: J. B. Blackmon
W. H. P. Drummond
R. L. Gervais
D. A. Steinmeyer
James H. Nourse
R. H. McFee
John Raetz

Martin Marietta
P. O. Box 179
Denver, CO 80201
Attn: T. R. Heaton
Lloyd Oldham
Tom Tracey
John Montague
Bill DeRocher
Dick Parker

Northrup Inc., Blake Laboratory
Suite 306
7061 S. University Blvd
Littleton, CO 80122
Attn: Floyd Blake
Jerry Anderson

Boeing Engineering & Construction
P. O. Box 3707
Seattle, WA 98124
Attn: Roger Gillette
J. R. Gintz

Westinghouse Corp.
Box 10864
Pittsburgh, PA 15236
Attn:. R. W. Devlin
J. J. Buggy
Mel Lipner

Northrup Inc.
302 Nichols Dr.
Hutchins, TX 75141
Attn: J. H. McDowell
J. A. Pietsch

University of Minnesota
Dept. of Electrical Eng., 139
129 Church St., SE
Minneapolis, MN 55455
Attn: Dr. Mahmoud Riaz

C-E Power Systems
Combustion Engineering, Inc.
1000 Prospect Hill Rd.
Windsor, CT 06095
Attn: C. R. Bozzuto

Arthur D. Little, Inc.
1 Maritime Plaza
San Francisco, CA 94111
Attn: John F. Butterfield

E-Systems
P. O. Box 226118
Dallas, TX 75266
Attn: Robert Walters

TRAC
1608 Colonial Terrace
Arlington, VA 22209
Attn: Ronald J. Thomas

Schumacher & Assoc.
Suite 120, 2550 Fair Oaks Blvd.
Sacramento, CA 95825
Attn: John C. Schumacher
Jeff Hansen

Exxon Enterprises - Solar Thermal Systems
P. O. Box 592
Florham Park, NJ 07932
Attn: Bob Garman
George Yenatchi

Energy Systems Group
Rockwell International
8900 DeSoto Ave.
Canoga Park, CA 91304
Attn: Tom Springer

General Motors Technical Center
Transportation Systems Div.
Warren, MI 48090
Attn: John Britt

Foster Wheeler
12 Peach Tree Hill Rd.
Livingston, NJ 07039
Attn: A. C. Gangadharan

Bechtel National Inc.
M/S 50/16
P. O. Box 3965
San Francisco, CA 94119
Attn: Ernie Lam
Robert L. Lessley

Ford Aerospace
3939 Fabian Way, T33
Palo Alto, CA 94303
Attn: I. E. Lewis
Howard Sund

Veda, Inc.
400 N. Mobil Bldg. D
Camarillo, CA 93010
Attn: Walter Moore

Veda, Inc., Suite 708
1755 S. Jefferson Davis Hwy.
Arlington, VA 22202
Attn: Ronald Bentley

Pittsburgh Corning
800 Presque Isle Dr.
Pittsburgh, PA 15239
Attn: David Rostoker

Springborn Laboratories
Water St.
Enfield, CT 06082
Attn: Bernard Baum
R. E. Cambron

Solar Energy Research Inst.
1536 Cole Blvd.
Golden, CO 80401
Attn: Charles J. Bishop
Barry Butler
James W. Doane
Ann Herlevich
Dennis Horgan
John Thornton
Neil Woodley

Electric Power Research Institute
P. O. Box 10412
Palo Alto, CA 93403
Attn: John Bigger
Piet Bos
John Cummings

Battelle Pacific NW Laboratories
P. O. Box 999
Richland, WA 99352
Attn: Kirk Drumheller
Michael A. Lind

University of Houston
Solar Energy Laboratory
Houston, TX 77004
Attn: A. F. Hildebrandt
Fred W. Lipps
Lorin Vant-Hull

Jet Propulsion Laboratory
4800 Oak Grove Dr.
Pasadena, CA 91003
Attn: Lewis Leibowitz
Vince Truscello
Tosh Fujita
James Bowyer

PRC Energy Analysis Co.
7600 Old Springhouse Rd.
McLean, VA 22101
Attn: R. B. Edelstein

Bureau of Reclamation
Code 1500 E
P. O. Box 25007
Denver, CO 80225
Attn: Stanley Hightower
Harry Remmers

MIT Lincoln Laboratory
M/S I-213
P. O. Box 73
Lexington, MA 02173
Attn: Philip Jarvinen

Aersopace Corp.
Solar Thermal Projects, Energy Systems Group
P. O. Box 92957
Los Angeles, CA 90009
Attn: Elliott L. Katz

Black & Veatch
P. O. Box 8405
Kansas City, MO 64114
Attn: John Kintigh
Sheldon Levy
Michael L. Wolf

Public Service of New Mexico
P. O. Box 2267
Albuquerque, NM 87103
Attn: Jack Maddox

Southern California Edison
2244 Walnut Grove
Rosemead, CA 91770
Attn: J. N. Reeves

Solar Thermal Test Facilities Users Assoc.
Suite 1204, First National Bank, East
Albuquerque, NM 87108
Attn: Frank Smith

Sun Power Corp.
55 Miller St.
Fairfield, CT 06430
Attn: Carl Whiteford

Westinghouse Electric Corp.
East Pittsburgh, PA 15112
Attn: John T. Day

PFR Engineering
4676 Admiralty Way, Suite 832
Marina del Rey, CA 90291
Attn: Tzvi Rozenman

G. W. Braun, DOE/HQ
L. Melamed, DOE/HQ
G. M. Kaplan, DOE/HQ
J. E. Rannels, DOE/HQ
M. U. Gutstein, DOE/HQ
L. S. Levine, DOE/ETS
R. W. Hughey, DOE/SAN
S. D. Elliott, DOE/SAN
R. N. Schweinberg, DOE/STMPO
C. N. Vittitoe, 4231
A. Narath, 4000; Attn: J. H. Scott, 4700
G. E. Brandvold, 4710
B. W. Marshall, 4713
G. W. Mulholland, 4713
L. K. Matthews, 4713
R. H. Braasch, 4715
E. C. Boes, 4719
D. G. Schueler, 4719
V. L. Dugan, 4720
J. V. Otts, 4721
J. F. Banas, 4722
W. P. Schimmel, 4723
T. A. Dellin, 4723 (10)
J. A. Leonard, 4725
H. M. Dodd, 4744
K. W. Mitchell, 5133
A. C. Ratzel, 5512
J. R. Koteras, 5523
R. S. Claassen, 5800
R. B. Pettit, 5842
F. P. Gerstle, 5844
T. B. Cook, 8000; Attn: A. N. Blackwell, 8200
W. E. Alzheimer, 8120
C. S. Hoyle, 8122
R. J. Gallagher, 8124
B. F. Murphey, 8300; Attn: D. M. Schuster, 8310
G. W. Anderson, 8330
W. Bauer, 8340
D. Hartley, 8350
T. S. Gold, 8320
P. J. Eicker, 8326
J. J. Iannucci, 8326
M. J. Fish, 8326 (15)
L. Gutierrez, 8400
C. S. Selvage, 8420
R. C. Wayne, 8450
W. G. Wilson, 8451 (10)
T. D. Brumleve, 8451
W. R. Delameter, 8451
C. L. Mavis, 8451
H. Norris, 8451
S. G. Peglow, 8451
A. C. Skinrood, 8452

K. W. Battleson, 8452
J. C. Gibson, 8452
J. D. Fish, 8452
L. V. Griffith, 8452
J. D. Gilson, 8453
T. T. Bramlette, 8453
L. G. Radosevich, 8453
C. T. Schafer, 8453
F. J. Cupps, 8265
Publication and Information Division, 8265, for TIC (27)
3141 (2)
8266-2 (3)